

Gamma-ray spectra from capture of 2-eV to 3-keV neutrons by $^{181}\text{Ta}^\dagger$

M. L. Stelts* and J. C. Browne

Lawrence Livermore Laboratory, University of California, Livermore, California 94550

(Received 27 December 1976)

The spectra of γ rays from the capture of neutrons by ^{181}Ta were measured at the Livermore 100-MeV linac for neutrons from 2 eV to 3 keV with a Ge(Li)-NaI three-crystal spectrometer. Neutron resonances were resolved to 200-eV neutron energy. Individual primary γ -ray transitions to final states in ^{182}Ta were resolved to 1778-keV excitation energy. These transitions were used to place 110 states with spin and parity assignments in the ^{182}Ta level diagram. A set of 1240 $E1$ transition strengths was extracted from 19 neutron resonances of known spin and parity. The most likely χ^2 fit to the distribution of these widths yielded 1.38 ± 0.11 degrees of freedom. The $E1$ transition strengths were also examined for correlations with the reduced neutron widths of the initial and final states. The $E1$ strength function was extracted for $E_\gamma = 4.3$ to 6.1 MeV and compared with previous results.

NUCLEAR REACTIONS $^{181}\text{Ta}(n, \gamma)$, $E = 2 \text{ eV} - 3 \text{ keV}$ measured $\sigma(E, E_\gamma)$, E_γ , I_γ ; deduced Q , ^{182}Ta levels; extracted $\Gamma_{\gamma i}$ distribution, strength function, correlation coefficients. Natural target, three-crystal Ge(Li)-NaI spectrometer.

I. INTRODUCTION

Neutron capture γ -ray measurements for the $^{181}\text{Ta}(n, \gamma)^{182}\text{Ta}$ reaction have been published previously by several authors.^{1,2} Reference 1 reported detailed spectral information for seven resolved resonances below 50 eV neutron energy using a single-crystal Ge(Li) detector. Reference 2 listed γ -ray spectra for the capture of neutrons in a 800-eV wide beam centered around 2 keV neutron energy also using a single-crystal Ge(Li) detector. Both measurements yielded spectroscopic information on the energies and spins and parities of final states in ^{182}Ta for excitation energies less than 1.24 MeV.

The present measurement improves on the earlier results by measuring the γ -ray spectra from neutrons captured by ^{181}Ta over the entire energy range from 2 eV to 3 keV using a three-crystal [Ge(Li)-NaI(Tl)] spectrometer. The excellent δ -function response of the detector allowed final states in ^{182}Ta to be assigned up to an excitation energy of 1.778 MeV. In addition to this spectroscopic information, a set of 1240 $E1$ transitions was obtained from 19 resonances of known spin and parity to determine its consistency with a Porter-Thomas distribution which is expected from a statistical description of the matrix elements involved in the deexcitation of the capture states.³ The $E1$ transition strengths were also examined for any correlation with the reduced neutron widths of either the initial or final states in ^{182}Ta . The γ -ray strength function for ^{182}Ta was also extracted for the γ -ray energy range from 4.3 to 6.1 MeV and is compared with previous re-

sults. The energy dependence of the strength function is examined to determine whether it is more consistent with an E_γ^3 dependence or with an E_γ^5 dependence, as predicted by the Brink-Axel hypothesis.⁴

II. EXPERIMENTAL TECHNIQUES

The experimental methods used in this experiment have been described in detail in previous reports^{5,6} so that only certain necessary aspects will be discussed here.

The capture γ -ray spectra for the $^{181}\text{Ta}(n, \gamma)$ reaction were measured using a three-crystal spectrometer [Ge(Li)-NaI] at the Livermore 100-MeV electron linac. The electron beam was stopped in a water-cooled tantalum target which served as the neutron source. The neutrons were moderated in a water-filled can which surrounded the target. The energy of the neutrons was determined by measuring their time of flight to the ^{181}Ta sample located 13.4 m from the neutron-producing target. The experimental facility is shown in Fig. 1. In this experiment, the electron beam parameters typically were 100 MeV energy, 100 nsec burst, 720 Hz repetition rate, and 100 μA average current. The sample was a 50-mm \times 100-mm sheet of natural tantalum (99.988% ^{181}Ta) with a thickness of 0.965 mm. The total running time was 75 h.

The three-crystal spectrometer consisted of a Ge(Li) central detector which was a true coaxial diode, 2 cm in diameter by 7.6 cm long (17.6 cm^3). This detector was sandwiched between two 127-mm diameter by 127-mm thick NaI(Tl) scintillators

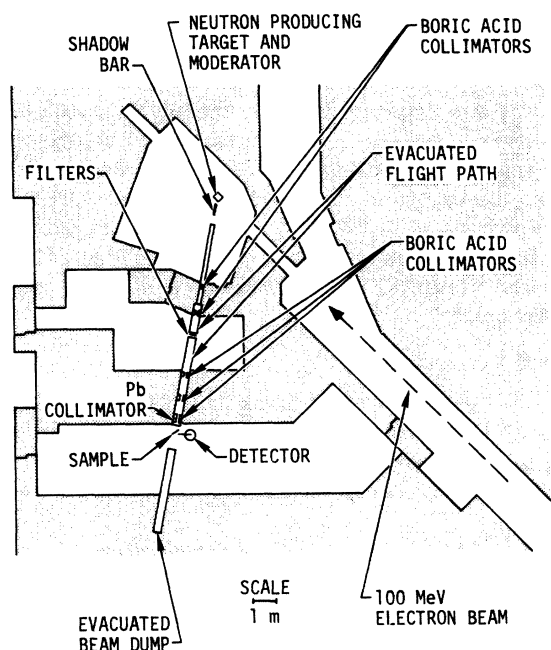


FIG. 1. The below-ground neutron time-of-flight facility at the Livermore 100-MeV electron linac.

and the whole assembly was enclosed in a combination bismuth and lead shield as shown in Fig. 2. The ${}^6\text{LiD}$ disc (152-mm diameter \times 12.7-mm thick) shown in Fig. 2 shielded the Ge(Li) detector from neutrons scattered by the Ta sample.

The detector peak efficiency was measured with calibrated γ -ray^{7,8} sources and thermal neutron capture γ rays from natural chlorine and chromium.⁹⁻¹¹ Since the effective interaction depth is a function of photon energy and since it is desirable to know the efficiency for all source-to-detector distances, the efficiency $\epsilon(E_\gamma, R)$ was measured both as a function of source energy and distance and parametrized as follows:

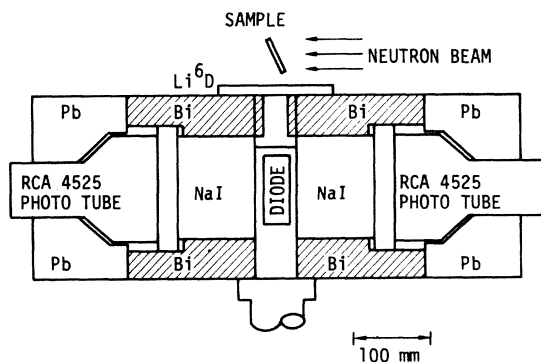


FIG. 2. Three-crystal spectrometer assembly showing the relative positions of the Ge(Li) diode, NaI scintillators, shielding, and sample.

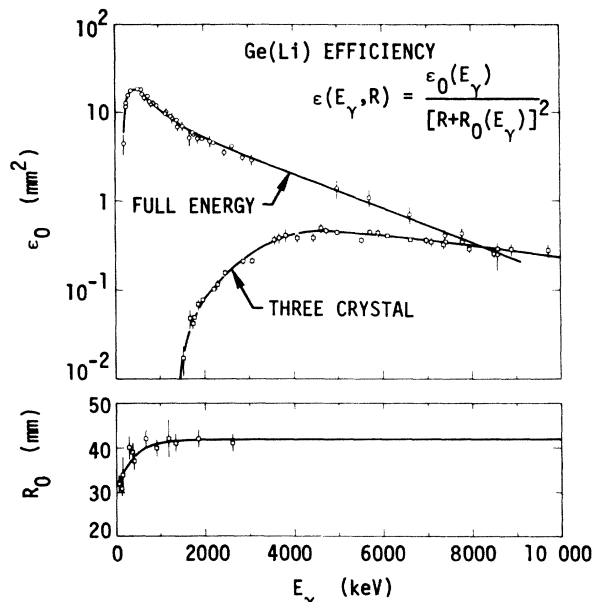


FIG. 3. Efficiency calibration for the Ge(Li) diode used in this experiment. The upper curve gives the parameter ϵ_0 , defined in the text, for the full-energy and three-crystal efficiencies. The bottom graph gives the effective interaction depth R_0 .

$$\epsilon(E_\gamma, R) = \epsilon_0(E_\gamma) / [R + R_0(E_\gamma)]^2,$$

where $\epsilon_0(E_\gamma)$ is the "intrinsic" efficiency in mm^2 , R is the distance from source to end cap, and R_0 the effective interaction depth measured from the end window. The results of the calibration are plotted in Fig. 3.

The operation of the Ge(Li) diode in the three-crystal coincidence mode reduces the efficiency for detection of the double-escape peak to 20% of the value of the diode alone due to the finite efficiency of the NaI detectors for photopeak detection of the 511-keV annihilation radiation. However, the peak-to-total-response ratio is improved from $\sim 1\%$ to $\sim 50\%$ using the triple coincidence method. The energy resolution of this system is 6 keV at 6 MeV γ -ray energy.

The data were accumulated via a PDP8/15 computer system into a two-dimensional array consisting of 624 neutron time-of-flight channels by 4088 γ -ray pulse-height channels and stored on a 3×10^6 18-bit word magnetic drum. These data were then transferred to magnetic tape for analysis.

III. EXPERIMENTAL RESULTS

The data were sorted into two groups for analysis. The first group consisted of a set of γ -ray spectra for 19 resolved neutron resonances of

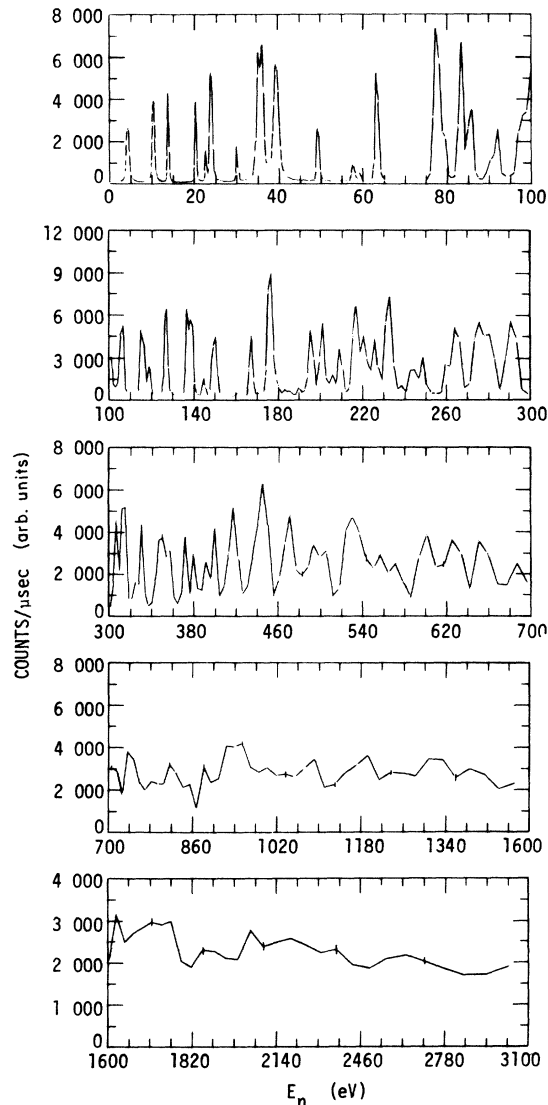


FIG. 4. Neutron time-of-flight spectrum as a function of neutron energy for γ -ray events depositing between 2.4 and 6.1 MeV in the three-crystal spectrometer.

known spin and parity. The second set consisted of γ -ray spectra summed over large bins of neutron energy in the range 20–3000 eV. From the first set, information was obtained on spins and parities of the final states in ^{182}Ta , the $E1$ strength function, and the statistical distribution of partial radiation widths of $E1$ transitions. The partial radiation widths from this set were also examined for correlations with the initial and final state reduced neutron widths. From the second set, information was obtained on the neutron energy dependence of the averaged primary intensities and the strength function.

The γ -ray counting rate as a function of neutron

energy is shown in Fig. 4. Sample γ -ray spectra for the 4.28-eV neutron resonance and for the neutron energy intervals from 20 to 100 and 100 to 200 eV are shown in Fig. 5. The energy calibration was established relative to natural chlorine thermal neutron capture lines,^{9–11} via the technique described in Ref. 5. Assuming the 6062.6-keV transition in the ^{181}Ta neutron capture data to be the transition to the ground state, the Q value for the $^{181}\text{Ta}(n, \gamma)$ reaction was determined by the relation

$$Q = E_\gamma + \frac{1}{2}E_\gamma^2/M_T c^2,$$

where $M_T c^2$ is the rest mass of ^{182}Ta . This yielded $Q = 6062.7 \pm 0.5$ keV, which is in agreement with the results of Wasson *et al.*¹ at 6063 ± 0.6 keV, and Helmer, Greenwood, and Reich² at 6062.9 ± 0.5 keV.

A. γ -ray spectra from resolved resonances

As a consequence of the Porter-Thomas fluctuations in the partial radiation widths, there is a high probability that any given transition in a given neutron resonance will have such a small width as to be unobservable. Therefore, the density of observable peaks should be smaller for isolated resonances than for spectra summed over many neutron resonances. This can be seen by comparing the spectra for the 4.28-eV resonance in Fig. 5 with the summed spectra. Consequently, if we analyze spectra from isolated resonances, peaks can be resolved to a much higher excitation energy. If the sample of isolated resonances is large enough, the probability of missing $E1$ transitions will be small. Table I lists the resonances analyzed individually. All were adequately resolved; published¹² values of the spins and parities were used in this analysis.

The γ -ray peak positions and areas were extracted using the method described in Ref. 5. The areas of the extracted peaks were converted to intensities via the following procedure. It was assumed that for a heavy nucleus such as Ta the capture spectrum is sufficiently complex that the total number of counts obtained by integration over a sufficiently large span of γ -ray energy should be proportional to the number of neutron capture events occurring in the sample. For each neutron resonance i the number T_i was extracted, where T_i was the sum of all counts in the channels which corresponded to the γ -ray energy range from 2.4 to 6.1 MeV. T_i was corrected for background and continuum events under the resonance. The intensity I_{if} for the transition from initial state i to final state f is given by

$$I_{if} = N \frac{A_{if}}{T_i \in (E_{\gamma if})}. \quad (1)$$

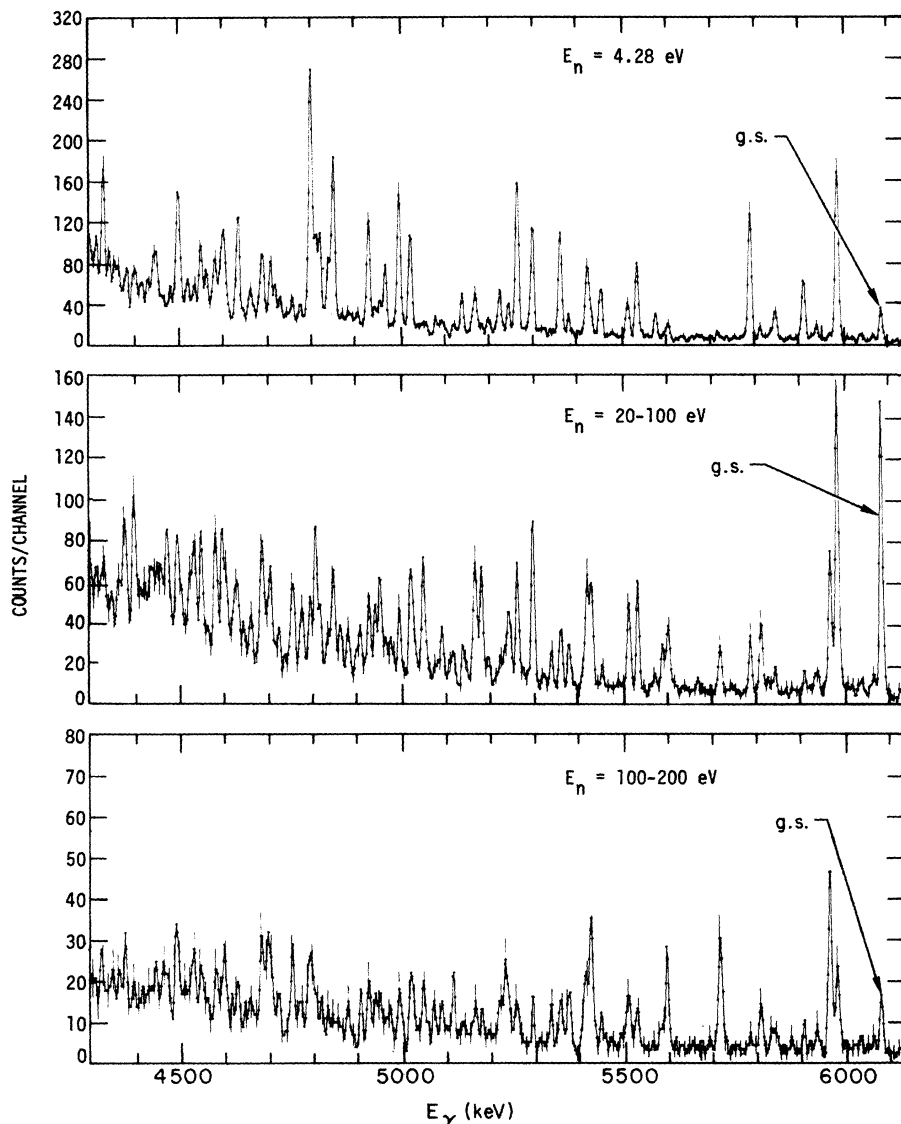


FIG. 5. Pulse-height spectra for the three-crystal spectrometer for the 4.28 eV resonance and the neutron energy regions, 20 to 100 eV, and 100 and 200 eV. The ground state (g.s.) transitions are indicated. The energy calibration is 2.29 keV/channel.

Here, A_{if} is the area of the peak at energy $E_{\gamma if}$. $\epsilon(E_{\gamma if})$ is the detector efficiency shown in Fig. 3. N is a constant chosen to normalize the sum of the intensities of the 6063-, 5965-, 5889-, and 5770-keV transitions of the 4.28-eV neutron resonance to the values of Ref. 13. The values of Ref. 13 were determined by measuring the intensities of these lines relative to several well-known lines in the $^{197}\text{Au}(n, \gamma)$ spectrum for the 4.9-eV resonance.^{14, 15}

The average partial radiation width for a transition of multipolarity L from initial state $J_i^{\pi_i}$ to final state $J_f^{\pi_f}$ can be expressed¹⁶ as

$$\bar{\Gamma}_{XLif} \propto D_{J_i^{\pi_i}}^{\pi_i} E_{\gamma if}^{2L+1},$$

where X is either E (electric) or M (magnetic), and $D_{J_i^{\pi_i}}^{\pi_i}$ is the level spacing of the initial states of spin and parity $J_i^{\pi_i}$. For γ -ray energies around 6 MeV, empirical estimates¹⁶ are that $M1$ partial radiation widths are approximately $\frac{1}{10}$ the $E1$ widths, and higher multiplicities are orders of magnitude lower still for this region in the Periodic Table. It is therefore reasonable to define a partial strength function S_{if} for dipole radiation as

$$S_{if} = \frac{I_{if} \Gamma_{if}}{D_{J_i^{\pi_i}} E_{\gamma if}^3}, \quad (2)$$

TABLE I. List of 19 resonances analyzed for resolved transitions.

| | E_0 (eV) | J^π | $2g\Gamma_n$ (meV) |
|----|------------------|-----------|----------------------------|
| 1 | 4.28 | 4* | 4.4 |
| 2 | 10.34 | 3* | 4.08 |
| 3 | 13.95 | 4* | 1.14 |
| 4 | 20.3 | 3* | 1.15 |
| 5 | 23.9 | 4* | 6.5 |
| 6 | 30.0 | 3* | 0.22 |
| 7 | 35.2 | 3* | 9.3 |
| 8 | 35.9 | 4* | 16.9 |
| 9 | 39.1 | 4* | 44.9 |
| 10 | 49.2 | 3* | 1.05 |
| 11 | 63.1 | 4* | 5.8 |
| 12 | 82.9 | 4* | 14 |
| 13 | 99.32 | 3* | 115 |
| 14 | { 103.5 105.5 | { ? 3* | { 1.1 } ^a 30 |
| 15 | 115.1 | 4* | 41 |
| 16 | 126.5 | 3* | 8.5 |
| 17 | 166.4 | 4* | 112 |
| 18 | 194.8 | 4* | 40 |
| 19 | 200.0 | 3 | |

^a Because of the large ratio of $2g\Gamma_n$, this was treated as a single 3* resonance.

where Γ_γ is the total radiative width of the compound state. For $^{181}\text{Ta} + n$, only 3* and 4* initial states in ^{182}Ta can be populated from the ($\frac{7}{2}$)⁺ ground state of ^{181}Ta by s-wave neutrons. Therefore, by averaging S_{if} over the 3* and 4* initial states, respectively, there should occur three groups of average S_{if} , depending on whether the transition can proceed by E1, M1, or only higher order multipole transitions. Thus if $\bar{S}(3^+ \rightarrow 2^-, 3^-, 4^-) = \bar{S}(4^+ \rightarrow 3^-, 4^-, 5^-) = 1$, then $\bar{S}(3^+ \rightarrow 2^+, 3^+, 4^+) = \bar{S}(4^+ \rightarrow 3^+, 4^+, 5^+) \sim 0.1$, and $\bar{S}(3^+ \rightarrow 5^+) = \bar{S}(4^+ \rightarrow 2^+) \sim 0.0$. Therefore, determinations as to whether the final state spin and parity is 2[±], (3,4)[±], or 5[±] can be made. The experimentally measured level spacing for 3* and 4* states is 4.4 ± 0.3 eV.¹² If it is assumed that the level density ρ_J in ^{182}Ta for states of spin J can be expressed as

$$\rho_J = (2J + 1)\rho_0(E) \quad (3)$$

and

$$D_J = 1/\rho_J,$$

then $D_3 = 10.1$ eV and $D_4 = 7.82$ eV, where D_3 and D_4 are the level spacings for $J=3$ and $J=4$ states, respectively. The quantity $\rho_0(E)$ describes the excitation energy dependence of the level density. The experimentally determined Γ_γ for neutron resonances in ^{182}Ta is (55 ± 2) meV.¹² Therefore, S_{if}

in Eq. (2) can be expressed as

$$S_{3f} = \frac{5.45 \times 10^{-6}}{E_{\gamma if}^3} I_{3f} \text{ MeV}^{-3} \quad (4a)$$

and

$$S_{4f} = \frac{7.05 \times 10^{-6}}{E_{\gamma if}^3} I_{4f} \text{ MeV}^{-3}, \quad (4b)$$

where the intensities are expressed in photons/1000 captures and $E_{\gamma if}$ is in MeV.

The set of intensities I_{if} was extracted from the resonance data by fitting to each of the 19 resonances all the γ -ray lines found in any of the 19 resonances listed in Table I, plus lines found in the background.

Table II lists the excitation energy, spin, and parity of each level which was observed in this experiment below an excitation energy of 1778 keV in ^{182}Ta . Also listed is the average value of \bar{S}_{3f} and \bar{S}_{4f} for each level from which the spin and parity assignment was deduced as discussed above. The level scheme of Ref. 2 is also given in Table II. The uncertainties in the excitation energies were determined by the least-squares fitting program, or set to 0.5 keV, whichever was larger. A discussion of the ^{182}Ta level scheme will be given in Sec. IV.

B. Averaged neutron γ -ray spectra

In addition to the 19 resolved neutron resonances, the γ -ray spectra were summed over the neutron energy groupings: 20 to 100 eV, 100 to 200 eV, 200 to 400 eV, 600 to 1000 eV, and 1000 to 3000 eV. γ -ray peak areas and centroids were extracted by automatic peak-fitting routines⁵ for these groups. The data were converted to energies and photons/1000 captures in the same manner as for the resolved resonance data.

Twelve transitions, not seen in the resolved resonance data, were observed in one or more of the averaged spectra. They are indicated with a "c" following the energy in Table II. Two of these transitions are to 4* final states observed by Helmer *et al.*² The rest are assumed to be positive parity states also, but no J^π assignments were attempted. In some instances, where there was not a clear distinction between E1 and M1 transition strengths in the resolved resonance data, a distinction could be made from the intensities of the averaged data. These levels are indicated in Table II by an "e" following the recommended J^π value.

IV. DISCUSSION

A. ^{182}Ta level scheme

Table II lists the excitation energies, spins, and parities of all the final states in ^{182}Ta that were ob-

TABLE II. Levels in ^{182}Ta observed in this experiment along with the average strength from 3^+ and 4^+ resonances. The most probable J^π is underlined.

| E_x (keV) | ΔE (keV) | Present results | | | Helmer <i>et al.</i> ^a | |
|--------------------|---------------------|---|---|----------------------------|-----------------------------------|---------------------------------|
| | | \bar{S}_{3f} ($\text{MeV}^{-3} \times 10^7$) | \bar{S}_{4f} ($\text{MeV}^{-3} \times 10^7$) | J^π | E_x (keV) | J^π |
| 0.0 | | 1.74 | 1.28 | <u>3, 4⁻</u> | 0 | 3 ⁻ |
| 16.9 | 0.7 | <0.01 | 0.10 | 5 [*] | 16.5 | 5 [*] |
| (90.2) | 1.7 | 0.04 | <0.01 | 3, 4, 5 ⁺ | <i>U</i> ^b | |
| 98.2 | 0.5 | 2.35 | 2.16 | <u>3, 4⁻</u> | 97.8 | 4 ⁻ |
| 114.6 | 0.5 | 1.62 | 1.09 | 3, 4 ⁻ | 114.33 | 4 ⁻ |
| 149.9 ^c | 1.1 | | | | 150.4 | 4 ⁺ |
| <i>U</i> | | | | | 163.3 | 6 ⁺ |
| 173.0 | 0.5 | <0.01 | 0.40 | 5 ⁻ | 173.4 | 5 ⁻ |
| 237.3 | 0.5 | 0.07 | 0.62 | 5 ⁻ | 237.37 | 5 ⁻ |
| 245.8 ^c | 1.6 | | | | <i>U</i> | |
| 251.5 | 1.0 | 0.17 | 0.15 | 3, 4 ⁺ | 250.2 | 3 ⁺ |
| 270.1 | 0.5 | 0.98 | 0.19 | <u>2⁻, 3, 4</u> | 270.4 | 2 ^{-d} |
| 292.5 | 0.4 | 0.05 | 0.93 | 5 ⁻ | 292.97 | 5 ⁻ |
| <i>U</i> | | | | | 317 ⁱ | 6 ⁻ |
| <i>U</i> | | | | | 331.4 | 5 ⁺ |
| <i>U</i> | | | | | 334.8 | 7 ⁺ |
| 359.6 | 1.3 | 0.28 | 0.25 | 3, 4 ^{-e} | 360.53 | 3 ⁻ |
| 365.5 | 1.3 | 0.11 | 0.15 | 3, 4 ⁺ | <i>U</i> | |
| <i>U</i> | | | | | 397.3 | 6 ⁺ |
| <i>U</i> | | | | | 402.65 | 2 ⁺ |
| <i>U</i> | | | | | 423.5 ^f | 2 ⁺ , 5 ⁺ |
| 458.2 ^c | 1.2 | | | | <i>U</i> | |
| <i>U</i> | | | | | 474.7 | 3 ⁺ |
| 477.4 | 0.5 | 1.15 | 0.67 | 3, 4 ⁻ | 479.8 | 4 ⁻ |
| 491.0 | 1.4 | 0.60 | 0.09 | 2 ⁻ | 491.8 | 2 ⁻ , 5 ⁻ |
| 505.4 | 0.6 | <0.01 | 0.16 | 5 ⁺ | 505.4 | 5 ⁺ |
| <i>U</i> | | | | | 519.7 | 10 ⁻ |
| 547.0 | 0.5 | 0.61 | 0.61 | 3, 4 ⁻ | 547.1 | 3 ⁻ |
| <i>U</i> | | | | | 559 | 1 ⁻ |
| 566.5 | 0.5 | 0.94 | 0.49 | 3, 4 ⁻ | 565.7 | 3, 4 ⁻ |
| 571.8 ^c | 2.2 | | | | 571.5 | 4 ⁺ |
| <i>U</i> | | | | | 584 | 0 ⁻ |
| <i>U</i> | | | | | 586.6 | 2 ⁺ , 5 ⁺ |
| 627.8 | 0.5 | 0.14 | 0.62 | 5 ⁻ | 628.4 | 5 ⁻ |
| 650.5 | 0.5 | 0.95 | 1.91 | 3, 4 ⁻ | 649 ^g | 4 ⁻ |
| 659.2 ^h | 0.5 | 1.27 | 0.51 | 2, 3, 4 ⁻ | 659.6 | 2 ⁻ |
| 662.8 ^c | 1.0 | | | | <i>U</i> | |
| 667.9 | 1.4 | 1.00 | <0.01 | 2 ⁻ | 666.0 | 2 ⁻ |
| 701.1 | 0.5 | 0.17 | 0.78 | 5 ⁻ | 702.0 | 3 ⁻ |
| 719.6 | 0.5 | 0.93 | 0.40 | 3, 4 ⁻ | 719.6 | 3 ⁻ |
| 740.9 | 0.9 | 0.72 | 0.18 | 2, 3, 4 ⁻ | 740.3 | 2 ⁻ |
| <i>U</i> | | | | | 777 ⁱ | 7 ⁻ |
| 781.9 | 0.5 | 0.06 | 2.46 | 5 ⁻ | 780.0 | 5 ⁻ |
| 791.0 ^c | 1.6 | | | | <i>U</i> | |
| 816.7 | 0.5 | 1.12 | 0.91 | 3, 4 ⁻ | 817.0 | 3 ⁻ |
| 830.5 ^c | 1.6 | | | | <i>U</i> | |
| 835.9 | 0.5 | 0.62 | 0.80 | 3, 4 ⁻ | 835.4 | 4 ⁻ |
| 842.0 | 1.2 | 0.25 | 0.74 | 3, 4, 5 ⁻ | 843.3 | 3, 4 ⁻ |
| 856.1 | 0.5 | 0.41 | 0.23 | 3, 4 ^{-e} | 856.0 | 2, 5 ⁻ |
| <i>U</i> | | | | | 866.3 | 2, 5 ⁻ |
| 881.2 | 0.8 | 0.03 | 0.20 | 3, 4, 5 ⁺ | 881.6 | 3, 4 ⁺ |
| 897.5 | 0.5 | 0.37 | 0.80 | 3, 4 ⁻ | 897.7 | 2, 5 ⁻ |
| 910.3 | 0.5 | 0.01 | 1.31 | 5 ⁻ | 910.0 | 3, 4 ⁻ |
| 914.7 | 0.5 | 0.73 | 0.78 | 3, 4 ⁻ | 915.7 | 2, 5 ⁻ |
| <i>U</i> | | | | | 935.8 | (2-5) ⁺ |
| 939.6 | 1.5 | <0.01 | 0.17 | 5 ⁻ | 939.9 | 2, 5 ⁻ |
| 960.0 | 1.5 | 0.24 | 0.29 | 3, 4 ^{-e} | 960.9 | 3, 4 ⁻ |

TABLE II. (Continued)

| E_x (keV) | ΔE (keV) | Present results | | | Helmer <i>et al.</i> ^a | |
|---------------------|---------------------|--|--|--------------------|-----------------------------------|------------------|
| | | \bar{S}_{3f} (MeV ⁻³ × 10 ⁷) | \bar{S}_{4f} (MeV ⁻³ × 10 ⁷) | J^π | E_x (keV) | J^π |
| 985.6 | 0.5 | 0.74 | 0.38 | 3,4 ⁻ | 986.6 | 3,4 ⁻ |
| 999.8 | 0.8 | 0.27 | 0.20 | 3,4 ⁻ | 1003.4 ^j | 2,5 ⁻ |
| 1021.6 | 1.5 | 0.16 | 0.07 | 3,4 ^{+e} | <i>U</i> | |
| 1028.4 | 0.6 | 1.81 | 0.25 | 3,4 ⁻ | 1029.4 | 3,4 ⁻ |
| 1049.9 | 0.9 | 0.56 | 0.54 | 3,4 ⁻ | 1050.5 | 3,4 ⁻ |
| 1056.6 | 0.5 | 0.85 | 1.13 | 3,4 ⁻ | 1057.7 | 3,4 ⁻ |
| 1082.0 | 0.5 | 0.55 | 1.45 | 3,4 ⁻ | 1082.6 | 3,4 ⁻ |
| 1101.2 | 0.8 | 0.02 | 0.39 | 5 ⁻ | 1100.7 | 2,5 ⁻ |
| 1113.6 | 0.5 | 0.20 | 1.10 | 5 ⁻ | 1113.5 | 2,5 ⁻ |
| 1125.0 ^c | 1.5 | | | | 1125.1 | 2,5 ⁻ |
| 1136.9 | 0.6 | 0.27 | 0.38 | 3,4 ⁻ | 1137.2 | 2,5 ⁻ |
| 1150.4 | 0.5 | 0.45 | 0.60 | 3,4 ⁻ | 1150.3 | 2,5 ⁻ |
| 1170.4 | 0.6 | 0.31 | 1.06 | 3,4 ⁻ | 1169.6 | 2,5 ⁻ |
| 1196.0 | 1.0 | 0.73 | 0.29 | 2,3,4 ⁻ | 1197.9 | 3,4 ⁻ |
| 1203.1 | 1.8 | 0.27 | 0.27 | 3,4,5 ⁺ | <i>U</i> | |
| 1216.1 | 1.1 | 0.52 | 0.05 | 2 ⁻ | 1216.3 | 2,5 ⁻ |
| 1229.7 | 0.5 | 0.30 | 1.77 | 3,4 ⁻ | 1229.8 | 3,4 ⁻ |
| 1240.4 | 0.5 | 0.76 | 0.39 | 3,4 ⁻ | 1240.4 | 2,5 ⁻ |
| 1260.1 | 0.5 | 0.97 | 0.30 | 3,4 ⁻ | 1259.4 | |
| 1269.5 | 0.5 | 0.35 | 1.74 | 3,4 ⁻ | 1270.3 | |
| 1279.8 | 0.5 | 0.42 | 1.94 | 3,4 ⁻ | 1281.1 | |
| 1284.4 | 0.5 | 0.71 | 0.47 | 3,4 ⁻ | <i>U</i> | |
| <i>U</i> | | | | | 1289.5 | |
| 1298.6 ^c | 1.0 | | | (2-5) | <i>U</i> | |
| 1302.5 | 0.6 | 0.33 | 0.70 | 3,4 ⁻ | 1303.5 | |
| 1321.0 | 1.5 | 1.56 | 1.04 | 3,4 ⁻ | 1322.5 | |
| 1326.0 | 2.2 | <0.01 | 0.80 | 5 ⁻ | <i>U</i> | |
| 1350.5 | 0.9 | 0.42 | 0.68 | 3,4 ⁻ | <i>U</i> | |
| 1360.4 | 0.8 | 0.15 | 0.60 | 5 ⁻ | <i>U</i> | |
| 1371.1 | 0.5 | 1.06 | 2.15 | 3,4 ⁻ | 1371.3 | |
| 1377.3 | 1.4 | 1.59 | 0.42 | 3,4 ⁻ | 1376.8 | |
| 1389.0 | 0.5 | 1.33 | 0.92 | 3,4 ⁻ | 1388.4 | |
| 1393.4 | 0.8 | 0.72 | 1.33 | 3,4 ⁻ | 1393.9 | |
| 1416.7 | 1.5 | 0.85 | 0.21 | 3,4 ⁻ | 1416.4 | |
| 1445.1 | 1.6 | 0.63 | 1.26 | 3,4 ⁻ | 1446.0 | |
| 1452.2 | 3.0 | 0.56 | 0.55 | 3,4 ⁻ | | |
| 1471.9 | 0.7 | 1.16 | 0.65 | 3,4 ⁻ | | |
| 1479.7 | 0.5 | 1.58 | 1.74 | 3,4 ⁻ | | |
| 1490.4 | 1.5 | 0.81 | 0.45 | 3,4 ⁻ | | |
| 1496.4 | 0.5 | 1.44 | 1.66 | 3,4 ⁻ | | |
| 1527.1 | 0.5 | 0.29 | 2.11 | 3,4 ⁻ | | |
| 1538.1 | 1.5 | 0.68 | 0.28 | 3,4,5 | | |
| 1541.7 | 0.6 | 0.77 | 0.82 | 3,4 ⁻ | | |
| 1545.6 | 2.3 | 0.53 | 0.23 | 2 ⁻ | | |
| 1551.6 | 0.5 | 0.01 | <0.71 | 5 ⁻ | | |
| 1555.7 | 0.8 | <0.01 | 0.95 | 5 ⁻ | | |
| 1570.8 | 1.2 | 0.49 | 0.12 | 2 ⁻ | | |
| 1577.2 | 0.8 | 1.20 | 0.93 | 3,4 ⁻ | | |
| 1582.3 | 0.6 | 1.35 | 2.23 | 3,4 ⁻ | | |
| 1604.9 | 1.7 | 0.60 | 1.91 | 3,4 ⁻ | | |
| 1612.0 | 0.8 | 0.74 | 0.42 | 3,4 ⁻ | | |
| 1617.5 | 2.5 | 2.5 | 1.11 | 3,4 ⁻ | | |
| 1628.3 | 0.8 | 0.40 | 1.55 | 3,4 ⁻ | | |
| 1635.6 | 0.8 | 0.52 | 0.54 | 3,4 ⁻ | | |
| 1641.8 | 1.5 | 0.59 | 0.97 | 3,4 ⁻ | | |
| 1646.1 ^c | 2.0 | | | (2-5) | | |
| 1650.5 | 2.7 | <0.01 | 0.87 | 5 ⁻ | | |

TABLE II. (Continued)

| E_x (keV) | ΔE (keV) | Present results | | | Helmer <i>et al.</i> ^a | |
|---------------------|---------------------|---|---|----------------------|-----------------------------------|---------|
| | | \bar{S}_{3f} ($\text{MeV}^{-3} \times 10^7$) | \bar{S}_{4f} ($\text{MeV}^{-3} \times 10^7$) | J^π | E_x (keV) | J^π |
| 1657.6 | 0.6 | 1.10 | 0.37 | 2, 3, 4 ⁺ | | |
| 1661.7 | 0.6 | 0.10 | 0.75 | 5 ⁻ | | |
| 1667.0 ^c | 1.5 | | | (2-5) | | |
| 1674.3 | 0.6 | 0.55 | 0.62 | 3, 4 ⁻ | | |
| 1679.6 | 0.5 | 0.98 | 1.18 | 3, 4 ⁻ | | |
| 1695.4 | 0.5 | 1.30 | 0.86 | 3, 4 ⁻ | | |
| 1701.1 | 1.5 | 0.55 | 1.13 | 3, 4 ⁻ | | |
| 1711.6 | 1.2 | 1.50 | 0.69 | 3, 4 ⁻ | | |
| 1724.7 | 0.9 | 0.38 | 0.58 | 3, 4 ⁻ | | |
| 1734.1 | 0.9 | 0.03 | 0.19 | 3, 4 | | |
| 1746.5 | 0.9 | 0.53 | 2.19 | 3, 4 ⁻ | | |
| 1756.3 | 1.4 | <0.01 | 0.16 | 5 ⁻ | | |
| 1762.5 | 1.2 | <0.01 | 0.63 | 5 ⁻ | | |
| 1765.9 ^c | 1.9 | | | (2-5) | | |
| 1769.6 | 1.0 | 0.22 | 0.01 | 3, 4 | | |
| 1778.3 | 1.2 | 0.56 | 0.63 | 3, 4 ⁻ | | |

^a Reference 2. Decay of ^{182}Hf , $^{182}\text{Ta}^m$, thermal capture, and 2 keV capture.

^b U designates an unobserved transition.

^c Seen only in averaged spectra.

^d There is probably an unresolved positive parity state at this excitation.

^e Parity assignment from averaged spectra.

^f Helmer *et al.* regard the existence of this level to be questionable.

^g Helmer *et al.* see possible splitting of this level.

^h The level at 662.8 seen in the averaged spectra probably contributes to this level.

ⁱ This level was observed in (d, p). The energies have been adjusted by Helmer *et al.* to correspond to their energy scale.

^j Helmer *et al.* see $E = 1000.4 \pm 0.5$ in thermal capture.

tained in this experiment. The results are compared in Table II with the results of Helmer *et al.*,² who studied the level structure of ^{182}Ta using the decay of ^{182}Hf to $^{182}\text{Ta}^m$, thermal neutron capture by ^{181}Ta and 2-keV (Scandium filter) neutron capture by ^{181}Ta with single-crystal Ge(Li) spectrometers. They have also included the $^{181}\text{Ta}(d, p)^{182}\text{Ta}$ results of Ref. 17 along with a private communication from Erskine in their proposed level scheme for ^{182}Ta .

1. Excitation energies

The present results are in reasonably good agreement with Helmer *et al.* in the region of overlap. A weak transition to a state at 90.2 keV was seen in the present resolved resonance data that was not seen by any of the previous investigators. The intensities for this line were at the threshold of observability except in the 4.28- and 20.9-eV 4^+ resonances. If the J^π of this state is 3^+ or 4^+ , a strong 90.2 $E1$ transition to the 3^- ground state would occur which is not consistent with the weak 90.1-keV transition observed in the low γ -ray energy thermal neutron capture data of Helmer

*et al.*² Therefore, the state, if it exists, probably has $J^\pi = 5^+$.

Other previously unreported states below 1250 keV, which were observed in the resonance data, occur at 365.5, 1021.6, and 1203.1 keV. These levels all have positive parity and the transitions populating them from the capture states are consequently weak. All of these transitions are within 8 keV of strong $E1$ transitions and could easily be missed in averaged spectral data with a spectrometer having less than excellent resolution, or lacking the clean response of a three-crystal spectrometer. Levels previously unreported in this excitation range were also observed at 245.8, 458.2, 662.8, 791.0, and 830.5 keV in the average spectra. Helmer *et al.*² reported levels with E , J^π of 331.3 keV, 5^+ ; 402.65 keV, 2^+ ; 423.5 keV, [2^+ , 5^+ (?)]; 474.7 keV, 3^+ ; 586.6 keV, [2^+ , 5^+ (?)]; 866.3 keV, ($2, 5^-$); and 935.8 keV, [($2-5$)⁺] from transitions in the 2-keV average neutron capture spectra that were not seen in the present results. (The "(?)" following the J^π means that Helmer *et al.* consider the existence of these levels in doubt.) With the exception of the 866.3-keV level,

these are all $M1$ transitions. All but the one to the 474.7-keV level have $J_f = 2^+$ or 5^+ and thus have only half the probability of being observed as a 3^+ or 4^+ state.

Wasson *et al.*¹ observed most of the allowable dipole transitions below the 1300-keV excitation seen in this experiment. They do report a level at 1054.2 keV which is not observed in either the work of Helmer *et al.*² or the present work. Above 1330-keV excitation, we were able to resolve transitions up to 1780 keV. Forty-one previously unreported levels were observed in this region.

2. Spins and parities

Spin and parity assignments for the states at 98.2, 114.6, and 270.1 keV were determined by Helmer *et al.*² by studying the β decay of ^{182}Hf to the 270.1-keV state and by measuring the γ decay branching ratios from this state. The assignments for the 519.7-, 334.8-, 163.3-, and 16.9-keV states were made by observing the cascade, branching ratios, and electron conversion spectra for the decay of the 16-min half-life 10^- isomer of $^{182}\text{Ta}^m$ at 519.7 keV. They extract further information on spins and parities of low-lying states by fitting the relative intensities of low energy transitions from thermal neutron capture to theoretical predictions. For final states with spins and parities in the range 2^\pm to 5^\pm , they examined the intensities of primary transitions from the capture of an 800-eV wide beam of 2-keV neutrons and, by assuming an E^5 γ -ray energy dependence for these intensities, extracted the relative strength function. By examining the relative strengths, the final state spins and parities could be determined to be $(3, 4)^-$, $(2, 5)^-$, $(3, 4)^+$, or $(2, 5)^+$. Some additional information came from the strengths of the $^{181}\text{Ta}(d, p)^{182}\text{Ta}$ reaction. They attempted to consolidate this information into a self-consistent level scheme using a rotational model with Coriolis coupling based on excitations of the deformed proton and neutron orbitals.

Up to an excitation energy of 668 keV there is excellent agreement between the present spin and parity assignments and those of Helmer *et al.* The states at 270.1 and 659.2 keV were assigned $J^\pi = 2^-$ by Helmer *et al.* However, we observed a definite strength for transitions to these states from 4^+ resonances which was consistent with $M1$ strength, while the strength from the 3^+ resonances was consistent with $E1$ strength. For the 659.2-keV state, an adjacent level of probably positive parity at 662.8 keV was observed in the average spectra. This state was not included in the fit of the resonance spectra and could explain the finite strength from the 4^+ resonances. Pos-

sibly there is also an unobserved positive parity level near 270-keV excitation.

Above 670 keV the agreement of spin and parity assignments between the present work and Helmer *et al.* is not as good. As excitation energy increases, the difficulty of making plausible assignments on the basis of nuclear models becomes increasingly difficult. Furthermore, above 840-keV excitation, they rely entirely on their 2-keV capture data to extract spins and parities. Since the Porter-Thomas fluctuations in their finite sample of capture states allow some overlap between sets of intensities for various combinations of final spin states, this disagreement is not unexpected.

B. Distributions of partial radiation widths

To determine the distribution of reduced partial widths for $E1$ transitions, a set of 1240 transitions was selected from the 19 resonances in Table I. Possible doublets were rejected, as were transitions to final states where the J^π assignments were in doubt. Since the raw partial widths $\Gamma_{J_i J_f}(E_{\gamma if})$ are functions of both γ -ray energy and the density of the initial states, the reduced partial widths were used. They are defined as the partial strength functions S_{if} in Eqs. (4).

The distribution of partial widths is expected to follow a χ^2 distribution with ν degrees of freedom. This distribution $p(s, \rho)$ is given by

$$p(s, \rho) = \frac{(\rho s)^{\rho-1}}{\Gamma(\rho)} e^{-\rho s}, \quad (5)$$

where $s = S_{if}/\bar{S}$, $\rho = \frac{1}{2}\nu$, $\Gamma(\rho)$ is the gamma function, and \bar{S} is the average of all S_{if} .

The method of analysis used for extracting ν was that of Perkins.¹⁸ He defines a *truncated* χ^2 distribution

$$P(s, \rho, \alpha) = \frac{F(\rho, \alpha)}{\Gamma(\rho)} (\rho s)^{\rho-1} \rho e^{-\rho s}, \quad \alpha \leq s < \infty, \quad (6)$$

where α is the point of truncation and

$$F(\rho, \alpha) = \frac{1}{\int_0^\alpha p(x, \rho) dx}. \quad (7)$$

The point of truncation α , was determined by the following method. The set of reduced errors $\{\epsilon_j\}$ was formed as

$$\epsilon_j = \Delta S_j / \bar{S},$$

where ΔS_j is the uncertainty for a particular transition strength and \bar{S} is the simple average of all S_j . Both the mean and the median of $\{\epsilon_j\}$ were computed. Then α was taken to be the lesser of the mean or median.

The likelihood function

$$L(\rho, \alpha) = \prod_{i=1}^N P(s_i, \rho, \alpha)$$

is then formed and the logarithmic derivative is set to zero to find the maximum likelihood. From the N values of $s_i \geq \alpha$ and tables calculated by Perkins, one can extract ν and $\Delta\nu$.

For our sample of 1240 $E1$ intensities this method yields $\nu = 1.38 \pm 0.11$. A fit to the data for this value of ν is shown in Fig. 6, where the data have been plotted as a function of the variable $x = \sqrt{s}$. $p(x, \nu)$ for $\nu=1$ and 2 have also been plotted. The distribution is clearly not fitted by $\nu=1$ or 2. The fit for $\nu=1.38$ is quite reasonable except for an excess of levels at $x \approx 1.8$. This bump cannot be fitted with any single χ^2 distribution.

Wasson *et al.*¹ extracted a ν from a set of 50 transitions from 9 resolved resonances giving a total sample of 450 transitions. Since they did not know the final state spins and parities they performed Monte Carlo calculations with a model assuming $M1$ and $E1$ transitions between states distributed with a $(2J+1)$ level density dependence for both initial and final states with the appropriate selection rules applying and compared these results with their data. They found $\nu = 0.75^{+0.23}_{-0.13}$ for the results of their analysis.

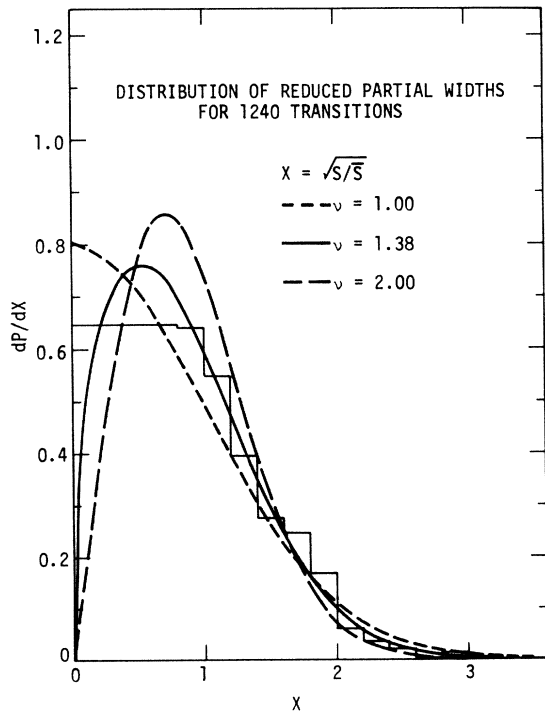


FIG. 6. The distribution of $E1$ partial radiation widths observed in this experiment. The differential distribution is plotted as a function of $x = (S/\bar{S})^{1/2}$. The maximum likelihood fit for χ^2 distribution with $\nu=1.38$ is plotted as well as the distributions for $\nu=1$ and $\nu=2$.

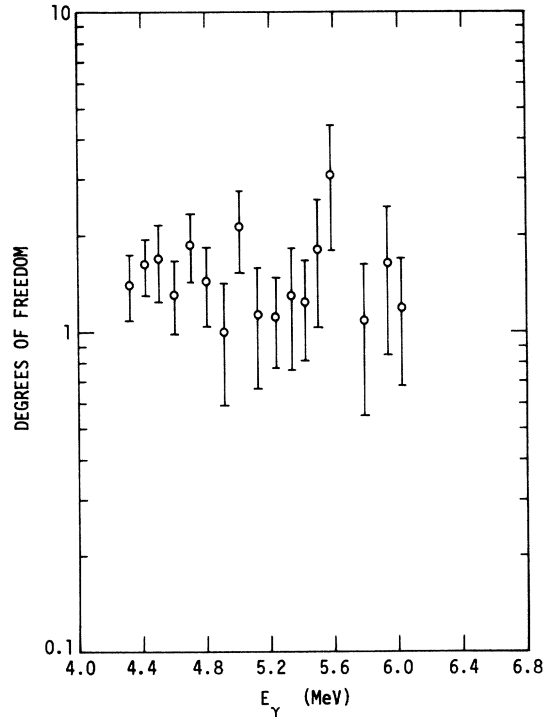


FIG. 7. The maximum likelihood values of the number of degrees of freedom for the $E1$ partial radiation widths divided into 100-keV bins as a function of γ -ray energy are shown.

Statistically, if the distribution for resolved transitions follows a χ^2 distribution with one degree of freedom, the distribution for an unresolved multiplet with n components will follow a χ^2 distribution with n degrees of freedom. To verify that the value of ν extracted in this experiment was not contaminated by unresolved $E1$ doublets, the data were subdivided into 100-keV bins in γ -ray energy and the fitting procedure repeated. The results are plotted as a function of E_γ in Fig. 7. Since the sample size is now much smaller, the variance of ν is much larger. The results are consistent with no energy dependence of ν and no increase in unresolved doublets as the excitation energy increases.

We also investigated the effect of the E_γ^3 dependence assumed in Eqs. (4) on the distribution of partial radiation widths. If we use an E_γ^5 dependence in Eqs. (4), we obtain a value for $\nu = 1.51 \pm 0.14$ which is consistent with the E_γ^3 result.

Since our $E1$ partial width distribution was drawn from a reasonably large set of neutron resonances (19) and included a large set of final states (60 for 3^+ resonances and 70 for 4^+ resonances), the departure from a Porter-Thomas distribution would appear to be significant. This deviation has also been observed for heavy nuclei by other

workers.¹⁹⁻²² It may be that this deviation from the statistical picture is indicative of nuclear structure effects. Beer²³ has proposed a theory for treating an anomalous width distribution but it does not provide any model for the nuclear structure effect involved. To determine if our $\nu = 1.38$ is indicative of nuclear structure effects, we have examined the data for correlations between the partial radiation widths and the reduced neutron widths of the initial and final states. This is discussed in the next section.

C. Correlation of γ -ray intensities

The existence of correlations between partial radiation widths and the reduced neutron widths of either the initial or final states has been reported by several authors (see Ref. 19). Various models have been invoked to explain these correlations. No attempt will be made to discuss any of these models. The reader is referred to several review articles for a complete description.^{19, 24, 25}

The low-lying states in ¹⁸²Ta have been described in Ref. 2 with the Nilsson model²⁶ as members of the rotational bands built on the intrinsic states resulting from the coupling of the odd proton and the odd neutron. In particular, the $K = 3^-$ and 4^- bands for the $\left\{\frac{7}{2}^+[404], \frac{1}{2}^-[510]\right\}$ configuration and the $K = 2^-$ and 5^- bands for the $\left\{\frac{7}{2}^+[404], \frac{3}{2}^-[512]\right\}$ configuration represent the majority of the low-lying unperturbed rotational bands. However, due to the Coriolis coupling of the $\frac{1}{2}^- [510]$ and $\frac{3}{2}^- [512]$ neutron orbitals, there is a significant amount of K mixing for these levels. Table III lists ten low-lying states in ¹⁸²Ta which were populated by primary transitions from the 3^+ and 4^+ resonances and also are described by the above configurations. The ¹⁸¹Ta(d, p) differential cross sections for these final states are also listed.

The reduced neutron widths $\Gamma_{n_i}^0$ for the nine 3^+ resonances and the ten 4^+ resonances listed in Table I were examined for correlations with the partial radiation widths to the ten final states listed in Table III. The linear correlation coefficient c for two variables x_i and y_i is defined by

$$c = \frac{\sum_i (x_i - \bar{x})(y_i - \bar{y})}{\left[\sum_i (x_i - \bar{x})^2 \sum_i (y_i - \bar{y})^2\right]^{1/2}}.$$

If we define the average correlation coefficient as $\bar{c}_R = (1/N) \sum_{j=1}^N c_{Rj}$, where $N = 6$ final states for the 3^+ resonances and $N = 9$ final states for the 4^+ resonances, we obtain $\bar{c}_R(3^+) = -0.12$ and $\bar{c}_R(4^+) = +0.03$. The probability (P_s) that a correlation coefficient equal to or greater than the above value could be generated by an equivalent set of random data is 0.40 and 0.81, respectively. Therefore, one must conclude that this is consistent with n_0

TABLE III. Low-lying states in ¹⁸²Ta used for correlation studies.

| E_x (keV) | J^π | $d\sigma/d\Omega^a$ ($\mu\text{b}/\text{sr}$) |
|----------------|---------|--|
| 0 | 3^- | 10.8 |
| 98 | 4^- | 7.1 |
| 115 | 4^- | 18.5 |
| 173 | 5^- | 10.4 |
| 237 | 5^- | 2.6 |
| 270 | 2^- | 5.8 |
| 293 | 5^- | 15.1 |
| 360 | 3^- | 7.8 |
| 477 | 4^- | 9.2 |
| 628 | 5^- | 1.4 |

^a Values are from Ref. 17.

correlation.

We also examined the data for correlations between the partial radiation widths and the reduced widths of the final states listed in Table III. For an odd- A target nucleus the (d, p) differential cross section can be expressed as²

$$d\sigma/d\Omega = \sum_{j_l} S_{j_l} \phi_{j_l},$$

where S_{j_l} is the spectroscopic factor, the ϕ_i are the intrinsic single-particle differential cross sections, and j and l are the total and orbital angular momentum of the captured neutron. The spectroscopic factor is defined as $\theta_{j_l}^2$, where θ_{j_l} is the reduced-width amplitude. With the Coriolis mixing, the final state wave function has an admixture of several K values so that the θ_{j_l} must be expressed as

$$\theta_{j_l} = \sum_K A_K \theta_{j_l, K},$$

where $\theta_{j_l, K}$ is the reduced width amplitude for a final state with a single K value and A_K is the admixed amplitude. Since there is this admixture of K values, we therefore decided that we would look for correlations between the *measured* quantity $d\sigma/d\Omega$ and the partial radiation widths rather than with the reduced width amplitudes $\theta_{j_l}^2$. With the set of final states restricted to those in Table III, the average correlation coefficient for the 3^+ resonances is $\bar{c}_r(3^+) = 0.27$ with $P_s = 0.05$, while for the 4^+ resonances $\bar{c}_r(4^+) = 0.19$ with $P_s = 0.07$. It should be pointed out that these correlation coefficients were also obtained if we assumed an E_γ^5 dependence in Eqs. (4) for the partial radiation width rather than E_γ^3 .

Therefore there is a significant correlation (at the 90-95% confidence level) between the partial radiation widths and the (d, p) differential cross

sections. We do not have an explanation for this correlation except to note that a similar effect has been noted in this mass region for ^{177}Hf (Ref. 21) and for the W isotopes (Ref. 22). The distribution of partial radiation widths for ^{177}Hf also deviates from a Porter-Thomas distribution with the number of degrees of freedom ν also equal to 1.38 (Ref. 21). It is interesting to note that the same neutron orbitals, $\frac{1}{2}^- [510]$ and $\frac{3}{2}^- [512]$, are involved in the low-lying states for these nuclei.

D. E1 strength function

The E1 strength function was computed by averaging the same set of partial strength functions from the 19 resolved resonances which were used in the determination of ν . Data were excluded from the average if the parity of the final state was in doubt or if a transition appeared to be a multiplet. The average strength function obtained in this manner is plotted in Fig. 8 using 100-keV averaging bins for the γ -ray energy. In this limited range of γ -ray energy, the results are consistent with an E_γ^3 dependence for the intensities with $\langle S \rangle = 9.1 \pm 0.5 \times 10^{-8} \text{ MeV}^{-3}$ over the entire data set. Least-squares fitting of the data to the function AE_γ^b gives an exponent $b = 2.52 \pm 0.61$, consistent with E_γ^3 . The dashed line in Fig. 8 is the least-squares fit to the data using an E_γ^5 dependence which is predicted by the Brink-Axel hypothesis.⁴

Figure 9 compares the strength function from the present experiment with the $^{181}\text{Ta}(n, \gamma)^{182}\text{Ta}$ data of Earle *et al.*,²⁷ which were obtained from measurements of the γ -ray spectra from capture of 0.7-MeV neutrons using NaI detectors, subsequent un-

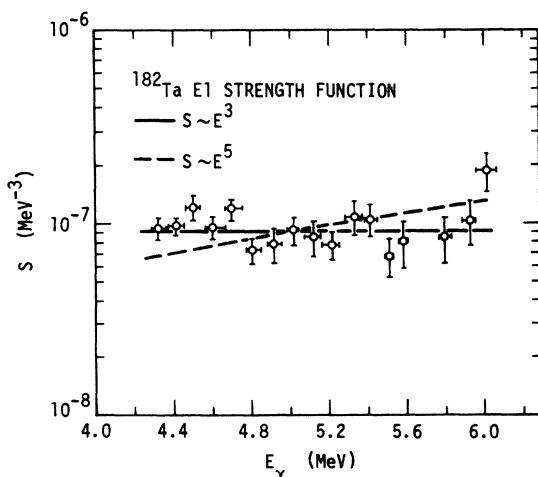


FIG. 8. The ^{182}Ta E1 strength function is plotted versus γ -ray energy. The least-squares fit of $\bar{S} = aE_\gamma^3$ is shown by the solid line and $\bar{S} = aE_\gamma^5$ by the dashed line.

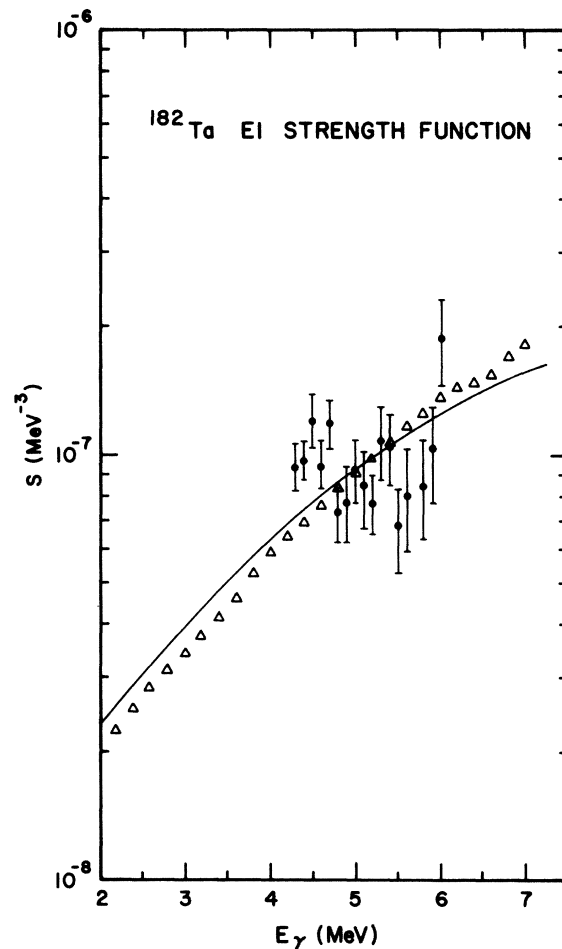


FIG. 9. Present results for the ^{182}Ta E1 strength function compared with the 0.7-MeV (n, γ) results of Earle *et al.* (Ref. 23) and the tail of the E1 giant resonance.

folding of the detector response, and correction for cascade γ rays. The present results are consistent with the absolute magnitude of their data. However, there is a discrepancy in the energy dependence, as can be seen in Fig. 9. The prediction of Bartholomew *et al.*,²⁸ based on the tail of the (γ, n) giant resonance, is shown as the solid line.

To assess the validity of our strength function it is necessary to look at two possible sources of systematic errors. The first is that of missing levels due both to the finite sample size and to the experimental sensitivity. We have sample sizes of nine and ten for the 3^+ and 4^+ resonances, respectively. If our sensitivity of detection is conservatively estimated to be 0.5 of the average E1 strength \bar{S} , then the upper limit for the number of E1 transitions missed is 11%. If all of the missing transitions have a strength equal to $0.5\bar{S}$, then our

strength function has been overestimated uniformly by about 5%. The second effect is due to the overlapping of levels at higher excitation energy. Above 1400 keV, the average level spacing for $(2-5)^-$ states is approximately 10 keV. Levels which are less than 2 keV apart most likely cannot be resolved experimentally. If we assume an exponential distribution for nearest neighbor spacings, then 18% of the levels listed for the higher excitation energies could be multiplets. If a 2^- and a 5^- level overlap we have made an incorrect spin assignment because both 3^+ and 4^+ resonances will show strength to the multiplet. However, such an overlap will not overestimate the average $E1$ strength since the value of \bar{S}_{3f} contains only the $3^+ \rightarrow 2^-$ $E1$ transitions and the value of \bar{S}_{4f} contains only the $4^+ \rightarrow 5^-$ $E1$ transitions. Now consider the remaining extreme assumptions. The first assumption is that we can ignore the effect of multiplets involving the overlap of either a 2^- or 5^- with a $(3, 4)^-$ because either \bar{S}_{3f} or \bar{S}_{4f} will be affected, but not both. This results in the average strength being overestimated by 2%. The other extreme condition is that we cannot ignore *any* multiplets (except those involving only a 2^- and 5^- for the reasons mentioned above). This results in the average strength being overestimated by 9%. The actual situation is probably intermediate between these two extreme assumptions. Therefore, the conclusion that can be drawn from this discussion is that the strength function as given in Fig. 8 may be overestimated by $\leq 10\%$ with the largest effect at the higher excitation energies. This possible source of systematic error tends to bring our results closer to those of Earle *et al.* in the 4-5 MeV γ -ray energy region, but it does not change our conclusion that our data are more consistent with E_γ^3 than E_γ^5 .

In addition to extracting a strength function from the resolved resonance data, the averaged neutron capture spectra discussed in Sec. III B were also analyzed to obtain information on the strength function. The data were analyzed assuming no prior knowledge of the energies of the $E1$ transitions. The ability to resolve transitions using averaged neutron capture data was reduced compared with the resolved resonance data because there is a higher effective γ -ray line density from averaging over the Porter-Thomas fluctuations. Also, there were poorer statistics and higher backgrounds as the neutron energy increased. For the average over the resonances in the neutron energy range $E_n = 20$ to 100 eV, all $E1$ transitions could be extracted up to 1200 keV excitation energy. However, for the average in the neutron energy range $E_n = 1000$ to 3000 eV, $E1$ transitions could be extracted only to 200 keV excitation.

Where the transitions could be resolved, the intensities from the averaged data agreed, to within the statistical limitations set by the Porter-Thomas fluctuations, with the average values from the resolved resonance data. The only exceptions were the transitions to the ground state and 98-keV state. Here the average intensity decreased as the neutron energy increased to a value consistent with the average strength function ($9.1 \times 10^{-8} \text{ MeV}^{-3}$) shown in Fig. 8.

These results were used to investigate the question of how well the strength function could be extracted from the averaged neutron capture data. If all transitions are assumed to be $E1$, a $2J+1$ level density dependence is assumed, and the dipole selection rules are used, it can be shown that

$$\bar{S}(E_\gamma) = \frac{2}{3} \frac{\Gamma_\gamma}{D} \frac{I(E_\gamma)\Delta E_\gamma}{N_\gamma E_\gamma^3} \text{ MeV}^{-3}. \quad (8)$$

Here $\bar{S}(E_\gamma)$ is the $E1$ strength function, Γ_γ is the total radiation width for capture of neutrons, D is the level spacing of the 3^+ and 4^+ capture states, $I(E_\gamma)$ is the average capture intensity (photons/1000 captures/MeV) in the bin which is ΔE_γ wide at E_γ , and N_γ is the total number of 2^- , 3^- , 4^- , or 5^- final states in the bin at the corresponding excitation energy. For the range of excitation energies in which the transitions could be resolved, the agreement with the resolved resonance data was within 30%. The range of γ -ray energy for which this can be done becomes severely limited in comparison with the resolved neutron resonance technique because of the high density of final states at high excitation.

V. SUMMARY

High resolution measurements of the spectra of γ rays from the capture of neutrons by ^{181}Ta were made in the neutron energy range from 2 eV to 3 keV. Ninety negative parity states were observed below 1.8 MeV excitation in ^{182}Ta . An additional 20 positive or undetermined parity states were also found in this excitation region. Spins were determined to be 2, (3, 4), or 5. Thirteen previously unreported states were observed below 1450 keV excitation. The measured level scheme is essentially consistent with previous work below 600 keV excitation, but the present results allow more reliable spin and parity assignments above this energy.

A set of 1240 $E1$ partial radiation widths was extracted from 19 resolved resonances of known spin and parity and fitted with a χ^2 distribution. The result of this analysis was $\nu = 1.38 \pm 0.11$ degrees of freedom, which is not consistent with the prediction of the extreme statistical model ($\nu = 1$). To determine whether this was owing to nuclear struc-

ture effects, the partial radiation widths were examined for correlations with the reduced neutron widths of the initial and final states. No correlations were found between the partial radiation widths and the initial state reduced neutron widths. However, a significant correlation between the partial radiation widths and the (d, p) cross sections for the low-lying final states in ^{182}Ta was obtained

for both 3^+ and 4^+ resonances.

The $E1$ strength function was extracted from both the resolved resonance data and the averaged neutron data. The energy dependence of the strength function was found to be more consistent with an E_γ^3 energy dependence over the 4.3 to 6.1 MeV γ -ray energy range rather than E_γ^5 as obtained in previous experiments.

†Work performed under the auspices of the U.S. Energy Research and Development Administration. W-7405-Eng-48.

*Now at Brookhaven National Laboratory, Upton, New York, 11973.

¹O. A. Wasson, R. E. Chrien, M. A. Lone, M. R. Bhat, and M. Beer, Nucl. Phys. **A132**, 161 (1969).

²R. G. Helmer, R. C. Greenwood, and C. W. Reich, Nucl. Phys. **A168**, 449 (1971).

³C. E. Porter and R. G. Thomas, Phys. Rev. **104**, 483 (1956).

⁴P. Axel, Phys. Rev. **126**, 671 (1962).

⁵M. L. Stelts and J. C. Browne, Nucl. Instrum. Methods **133**, 35 (1976).

⁶M. L. Stelts, Ph.D. thesis, Lawrence Livermore Laboratory Report No. UCRL-51907, 1975 (unpublished).

⁷W. W. Bowman and K. W. MacMurdo, At. Data Nucl. Data Tables **13**, No. 2-3 (1974).

⁸R. Gunnink, J. B. Niday, R. P. Anderson, and R. A. Meyer, Lawrence Livermore Laboratory Report No. UCID-15439, 1969 (unpublished).

⁹G. D. Loper and E. G. Thomas, Nucl. Instrum. Methods **105**, 453 (1972).

¹⁰L. B. Hughes and T. J. Kennett, Can. J. Phys. **48**, 1130 (1970).

¹¹V. J. Orphan, N. C. Rasmussen, and T. L. Harper, Gulf General Atomics Report No. GA-10248, DASA-2570, 1970 (unpublished).

¹²Resonance Parameters, compiled by S. F. Mughabghab and D. I. Garber, Brookhaven National Laboratory Report No. BNL-325 (National Technical Information Service, Springfield, Virginia, 1973), 3rd ed., Vol. 1.

¹³C. M. McCullagh, Brookhaven National Laboratory and State University of New York at Stony Brook (private communication).

¹⁴G. D. Loper, G. E. Thomas, and L. M. Bollinger, Nucl. Instrum. Methods **121**, 581 (1974).

¹⁵W. Kane, Brookhaven National Laboratory (private

communication).

¹⁶L. M. Bollinger, in *Experimental Neutron Resonance Spectroscopy*, edited by J. P. Harvey (Academic, New York, 1970), pp. 235-345.

¹⁷J. R. Erskine and W. W. Buechner, Phys. Rev. **133**, B370 (1964).

¹⁸S. T. Perkins, Lawrence Livermore Laboratory Report No. UCRL-51518, 1974 (unpublished).

¹⁹R. E. Chrien, in *Neutron Capture Gamma-Ray Spectroscopy*, proceedings of the international symposium on neutron-capture gamma-ray spectroscopy, Studsvik, Sweden, 1969 (IAEA, Vienna, 1969), pp. 627-649.

²⁰F. Becvar, R. E. Chrien, and O. A. Wasson, Nucl. Phys. **A236**, 198 (1974).

²¹M. Stefanon and F. Corvi, Nucl. Phys. **A281**, 240 (1977).

²²J. Murray, B. W. Thomas, and E. R. Rae, in *Neutron Capture Gamma-Ray Spectroscopy*, proceedings of the international symposium on neutron-capture gamma-ray spectroscopy, Studsvik, Sweden, 1969 (See Ref. 19), pp. 579-586.

²³M. Beer, Phys. Rev. **181**, 1422 (1969).

²⁴A. M. Lane, in *Neutron Capture Gamma-Ray Spectroscopy*, proceedings of the international symposium on neutron-capture gamma-ray spectroscopy, Studsvik, Sweden, 1969 (See Ref. 19), pp. 513-526.

²⁵S. F. Mughabghab, in *Neutron Capture Gamma-Ray Spectroscopy*, proceedings of the second international symposium on neutron capture gamma-ray spectroscopy and related topics, Petten, 1974 (Reactor Centrum Nederland, Petten, 1975), pp. 53-80.

²⁶S. G. Nilsson, K. Dan. Vidensk. Selsk. Mat.-Fys. Medd. **29**, No. 16 (1955).

²⁷E. D. Earle, M. A. Lone, G. A. Bartholomew, W. J. McDonald, K. H. Bray, G. A. Moss, and G. C. Neilson, Can. J. Phys. **52**, 989 (1974).

²⁸G. A. Bartholomew, I. Berquist, E. D. Earle, and A. J. Ferguson, Can. J. Phys. **48**, 687 (1970).

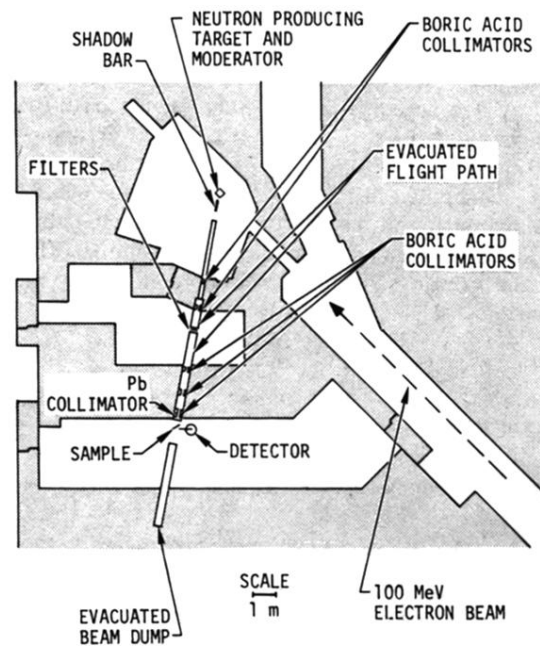


FIG. 1. The below-ground neutron time-of-flight facility at the Livermore 100-MeV electron linac.